

High-harmonic generation and correlated two-electron multiphoton ionization with elliptically polarized light

P. Dietrich, N. H. Burnett, M. Ivanov, and P. B. Corkum

Steacie Institute for Molecular Sciences, National Research Council of Canada, M-23A, Ottawa, Ontario, Canada K1A 0R6

(Received 21 May 1993; revised manuscript received 25 July 1994)

The strong ellipticity dependence of correlated two-electron multiphoton ionization of neon and of the high-harmonic emission from argon (harmonic $N=21$) and neon ($N=41$) are reported. These measurements suggest a common underlying mechanism and are quantitatively consistent with a recently developed Keldysh-like model of high harmonic generation which treats the interaction between a newly freed electron and the ion core.

PACS number(s): 42.50.Hz, 42.65.Ky, 32.80.Hd, 34.80.Dp

High harmonic generation [1,2] represents a potential practical source of coherent extreme ultraviolet (XUV) radiation. Based on semiclassical considerations, it has been proposed [3] that high harmonic generation and high-field (in the tunneling limit) correlated two-electron multiphoton ionization are closely related phenomena, both resulting from the interaction of electrons, that have been excited high into the continuum, with the parent ions. If these electrons recombine with the parent ion, they yield harmonic radiation; if they inelastically scatter, a second electron can be freed.

Here we experimentally examine the dependence of these phenomena on the ellipticity of the driving field. In the semiclassical model [3], it is possible to directly relate the ellipticity dependence of both phenomena to the rate of transverse spreading of the ionizing electron wave function. Our results are consistent with a common basis for these processes and with a transverse spreading of the electron wave function dictated by simple quantum-mechanical principles.

From very general principles we know that high-harmonic intensities must depend on the ellipticity ϵ of the laser field. As we will show, ellipticity measurements provide a direct test of models used to predict the nonlinear polarizability of ionizing gases, a test which is insensitive to phase matching.

Correlated two-electron multiphoton ionization has recently been reported in high-field multiphoton ionization experiments [4] in Ne and He. For the portion of our study that concentrates on correlated two-electron multiphoton ionization, we will follow the experimental procedure pioneered in these experiments and in much lower power experiments in Xe [5], but will concentrate on the ellipticity dependence.

As with experiments reported in [1,2,4] we focus on laser fields where the energy U_p of the electron oscillations in an electric field $E_0 \cos \omega t$ is larger than the binding energy I_p of the electron in the atom: $U_p \equiv e^2 E_0^2 / 4m\omega^2 \geq I_p$ (e and m are the electron charge and mass). The ionization process in such laser fields is well understood as optical tunneling, and various experiments [6,7] are described by the Ammosov-Delone-Krainov (ADK) tunneling formula [8]. Furthermore, the predictions of the quantum-mechanical ADK theory can be combined with classical trajectory calculations to develop a very useful semiclassical picture [3,6]. Thus our experiment is performed in the best understood of the multiphoton limits.

The ellipticity dependence of high-harmonic emission from Ne and Ar was studied with a compact all Ti:sapphire laser system. We refer the reader to a similar experiment that has recently been published [9]. The output of the cw mode-locked oscillator is amplified using chirped pulse amplification in a regenerative amplifier followed by a two-pass final amplifier to produce 10-mJ, 200-fs pulses at a repetition rate of 2 Hz and wavelength of 775 nm. After compression in a two-grating double-pass compressor the laser pulses are linearly polarized to better than 500:1 in intensity. Ellipticity is introduced by rotating a zero-order $\lambda/4$ waveplate placed just before the focusing lens and target chamber window. The pulses are focused by an $f/30$ thin lens onto a 3.1-mm-diam stainless-steel tube with 150- μm -thick walls which has been squeezed to an internal thickness of 750 μm . A 150- μm -diam hole is drilled by slightly defocusing the laser and irradiating the target for a few hundred shots. The laser is then focused to a 75- μm diameter for harmonic production. The laser intensity averaged over its 90% energy circle is estimated to be $8 \times 10^{14} \text{ W cm}^{-2}$. The target tube is transiently filled with approximately 100 mbar of Ar or Ne with a fast pulsed valve. The harmonic radiation is dispersed with a 1200-groove/mm Hitachi variable space grating with a slit placed in its focal plane to isolate one harmonic. Harmonic yield is monitored on an electron multiplier placed behind the slit. Rotating the $\lambda/4$ waveplate rotates the major axis of the polarization ellipse with respect to the plane of incidence of the diffraction grating. At the experimental angle of incidence (87°) the change in the diffraction efficiency due to this effect is negligible for the present purposes. Zero-order (specular reflection) radiation from the grating is collected and transmitted through a window to monitor the third-harmonic yield (by means of a grating spectrograph and UV photomultiplier).

Using this apparatus, harmonic radiation extending out to $N > 31$ has been observed in argon and $N > 41$ in neon. Harmonic yield as a function of the ellipticity ϵ is shown as data points in Fig. 1(a) for the 41st harmonic in neon and Fig. 1(b) for the 21st in argon. The curves plot theoretical results which will be discussed below.

To study two-electron multiphoton ionization we use the amplified output of a colliding-pulse mode-locked laser operated at 625 nm [10]. The 70-fs pulses are amplified in a

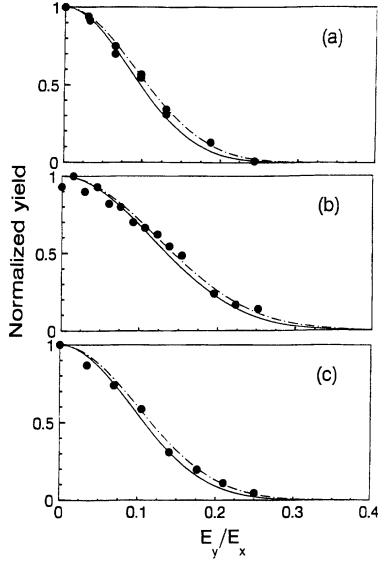


FIG. 1. Dependence of the intensity of the (a) 41st harmonic from Ne, (b) 21st harmonic from Ar, and (c) the correlated two-electron multiphoton ionization yield on the ellipticity $\varepsilon = E_y/E_x$. *Experimental parameters:* (a) and (b) pulse duration ~ 200 -fs laser pulses, $\lambda = 775$ nm, and peak intensity $\sim 8 \times 10^{14}$ W cm $^{-2}$; (c) pulse duration ~ 100 fs, $\lambda = 625$ nm, and peak intensity $\sim 9 \times 10^{14}$ W cm $^{-2}$. *Theoretical parameters:* (a) solid and dashed curves are for intensities of 8×10^{14} W cm $^{-2}$ and 5×10^{14} W cm $^{-2}$, respectively; (b) solid and dashed curves are for intensities of 3×10^{14} and 2×10^{14} W cm $^{-2}$, respectively; and (c) solid and dashed curves are for the lower and upper limit for R_{ion} from Eq. (4) calculated at 9×10^{14} W cm $^{-2}$.

dye-laser amplifier chain pumped by a frequency-doubled neodymium-doped yttrium aluminum garnet (Nd:YAG) laser and then compressed in a two-grating, single-pass compressor. A vacuum spatial filter combined with an aperture to select the central part of the Airy pattern ensures a good spatial profile. A small portion of the beam is sampled to measure the pulse energy and to produce second-harmonic radiation in a KDP crystal whose energy is also measured. The pulses have an energy of 150–200 μJ and a duration of about 100 fs measured with a single shot autocorrelator. Just before entering the vacuum chamber, the pulses pass through a linear polarizer and a $\lambda/4$ wave plate which can be rotated to change the ellipticity of the pulse. The residual ellipticity in the case of linear polarization is $\varepsilon \leq 0.02$.

The pulses are focused inside the time-of-flight mass spectrometer using an on-axis paraboloidal mirror with 50-mm focal length. We use $f/5$ focusing geometry resulting in a focal diameter of ~ 3 μm . Neon is leaked into the vacuum chamber with a background pressure of 6×10^{-9} mbar. The operating pressure was adjusted between 10^{-7} and 10^{-5} mbar depending on the pulse intensity. The ions are extracted by an electric field of 500 V cm $^{-1}$ and detected by a microchannel plate. The amplified signals are integrated using boxcar integrators. The signals from both ion channels were measured without neon in the chamber and subtract from the actual neon signals for background suppression. Furthermore we measured the boxcar output between laser pulses to correct for drifting offsets of the boxcar integrators.

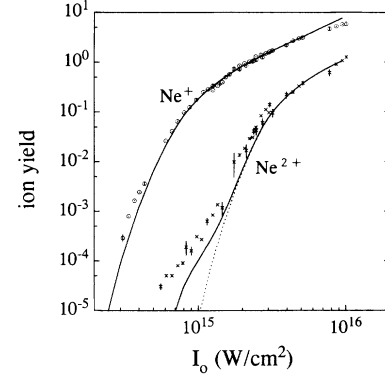


FIG. 2. Intensity dependence of the ion yield of neon with linearly polarized 625-nm light. The solid curves display the theoretical result for all charge states. The dashed curve is the result of calculations where only tunnel ionization is considered.

The experimental data from all pulses were binned according to their energy, $E_{1\omega}$, and discriminated on the basis of the energy of the second harmonic, $E_{2\omega}$. Only pulses with $\alpha = E_{1\omega}^2/E_{2\omega}$ within $\pm 10\%$ of a preset value were accepted. For pulses whose temporal shape can be described by one parameter τ , α is proportional to the pulse duration τ . This selection ensures the reproducibility of the data. Each data point shown in Fig. 2 is an average over typically 1000 shots. The error is the statistical error of the mean.

The intensity dependence of the ionization yields of Ne^{n+} ($n=1,2$) in the range 10^{14} – 10^{16} W cm $^{-2}$ for linear polarization is shown in Fig. 2. The intensity scale was obtained by fitting the experimental Ne^+ yields with the calculated yields from the tunnel ionization model by scaling both intensity and yields. The experimental data for Ne^{2+} show a clear bump at low yields. This increase of the ion yields compared to a simple tunnel ionization model is similar to published results, and it has been proposed that it is the result of two-electron multiphoton ionization [4]. The curves show theoretical results, which will be discussed below.

The Ne^+ and Ne^{2+} yields at a peak intensity of 9×10^{14} W cm $^{-2}$ were measured as a function of the ellipticity. Whereas the Ne^+ yields (not shown) do not vary significantly over the measured range, the Ne^{2+} yields decrease rapidly [data points in Fig. 1(c)]. The curves plot theoretical results that will be discussed below. The qualitative agreement between the different measurements in Fig. 1 lends strong support to the hypothesis that the underlying physics investigated by both diagnostics is the same.

The signal measured in any harmonic generation experiment is the result of the interplay between the nonlinear response of the atom and the phase matching. Phase-matching issues have been extensively studied [2] and there are two main sources of dephasing: (1) the natural phase advance that occurs in any beam as it passes through its geometric focus and (2) dispersion in the nonlinear medium. Both of these should be unchanged by the very small ellipticity characteristic of this experiment. Consequently, our ellipticity measurements must reflect changes in the atomic response. We now summarize the basic features of a semiclassical model of light-atom interactions [3], which predicts the common ellipticity dependence for both harmonic generation and

two-electron ionization, as observed in experiment.

In an intense laser field an atomic electron can tunnel through the barrier created by the superposition of the Coulomb potential of the atomic core with the instantaneous electric field $E(t_0) = E_0 \cos \omega t_0$ [8]. Tunneling may occur at any time t_0 , with the probability given by the tunneling formula [8] for a constant field $E(t_0)$. As a result, the electron appears in the continuum near the nucleus with initial velocity $v(t_0) \approx 0$ [3]. Its further motion is described by the Newton equation, which shows that the electron can return to the ion during the first cycle after birth [3,11]. If the electron recombines to the ground state when passing the ion at the moment t , it will emit a photon $\hbar\Omega = \mathcal{E}(t) + I_p$, where $\mathcal{E}(t)$ is the electron instantaneous kinetic energy calculated under the approximation that the Coulomb interaction can be ignored. In this approximation the maximum possible kinetic energy of the electron when passing the ion is $\mathcal{E}(t) = 3.17U_p$. For the intensities required for significant ionization of neon or helium with 0.6- μm light, this maximum possible kinetic energy is about 100 eV, sufficient to collisionally ionize (or excite) a second electron.

The semiclassical picture gives a very physical way of looking at the ellipticity dependence of strong-field processes. Consider an elliptically polarized laser field with the main component along the x axis, $E_x(t) = E_{0x} \cos \omega t$ and a weak perpendicular component $E_y(t) = E_{0y} \sin \omega t$ with ellipticity $\varepsilon \equiv E_{0y}/E_{0x} \ll 1$. Since the tunneling probability depends exponentially on the width of the potential barrier, the electron tunnels near the peak of the main field E_x , when $|\cos \omega t| \approx 1$. Consequently, by the time the electron can return to the ion, its displacement in the y direction from the origin is $\Delta y = [-\sin \omega t + \sin \omega t' + (\omega t - \omega t') \cos \omega t'] \varepsilon e E_{0x} / m \omega^2$, where t' is the moment when the electron is born in the continuum and t the time the electron returns to the ion. For electrons that return to the ion with high energies (close to $3U_p$) $\omega t' \sim 0.3$ and $\omega t - \omega t' \sim 4$, which gives $\Delta y \approx 5\varepsilon e E_{0x} / m \omega^2$. For laser intensity $I \sim 10^{15} \text{ W/cm}^2$, $\varepsilon \sim 0.1$ and ω in the optical frequency range, $\Delta y \sim 10 - 15 \text{ \AA}$. As a result, the electron can easily miss the ion and no high harmonics will be observed.

Quantum mechanically the initial kinetic energy of the electron in the continuum is not exactly zero and can compensate for the drift in y direction. In other words, the quantum-mechanical wave packet spreads in all directions. The semiclassical model predicts that high harmonics will disappear when the transverse displacement of the electron becomes larger than the spreading of the wave packet. In a fully quantum-mechanical generalization [12] of the semiclassical model [3] the spreading of the wave packet is completely accounted for when the Schrödinger equation is solved. We will therefore use the theory described in Ref. [12] to fit our experimental data.

Harmonic emission is determined by the corresponding Fourier components of the laser-induced dipole moment $\mathbf{d}(t) = \langle \Psi(t) | \mathbf{d} | \Psi(t) \rangle$. According to Ref. [12], the main contribution to high-harmonic components of this dipole moment comes from the overlap between the ground-state wave function $\Psi_g(t)$ and the part of the wave function excited to the continuum, $\Psi_c(t)$: $\mathbf{d}(t) = \langle \Psi_c(t) | \mathbf{d} | \Psi_g(t) \rangle + \text{c.c.}$ Furthermore, analyzing the expression for $\mathbf{d}(t) = \langle \Psi_c(t) | \mathbf{d} | \Psi_g(t) \rangle + \text{c.c.}$ obtained in [12] (see Sec. IV of

Ref. [12]), one immediately finds that the main contribution to the N th Fourier component of the dipole moment comes from the moments of time t_N at which the electron born at rest near the nucleus returns to the nucleus with the energy satisfying the condition $N\hbar\omega = I_p + \mathcal{E}(t_N)$. Therefore, a simple estimate for the relative strength of harmonic signal $R_N(\varepsilon) = I_N(\varepsilon)/I_N(\varepsilon=0)$ as a function of ellipticity can be obtained by calculating the positive-frequency part of the overlap integral $\mathbf{d}_+(t) = \langle \Psi_g(t) | \mathbf{d} | \Psi_c(t) \rangle$ at the appropriate moment of time t_N : $R_N(\varepsilon) \sim |\mathbf{d}_+(t_N, \varepsilon)|^2 / |\mathbf{d}_+(t_N, \varepsilon=0)|^2$. Basically, this ratio measures the relative number of electrons passing the origin within the distance given by the size of the ground-state wave function ($\sim 1 \text{ \AA}$). This ratio is plotted in Figs. 1(a) and 1(b). To obtain Figs. 1(a) and 1(b) we have used the fact that below the cutoff there are always two moments of time, $t_N^{(1)}$ and $t_N^{(2)}$, at which the electrons born during the first quarter-period ($0 < \omega t < \pi/2$) return to the parent ion with appropriate energy $\mathcal{E}(t_N) = N\hbar\omega - I_p$. The harmonic signal is determined by the interference of the contributions from these two moments. However, in experiments this interference pattern is always smeared out by the inhomogeneous intensity distribution in space and time. Therefore, for the simplicity in Figs. 1(a) and 1(b) we used the moment t_N which corresponds to the electrons born near the peak of the instantaneous field $E_x \cos(\omega t)$, where the probability of transition to the continuum is larger.

Since the intensity distribution of the fundamental is not uniform, in Fig. 1(a) we present two curves for the 41st harmonic of neon: the solid curve is for the peak intensity in the experiment ($8 \times 10^{14} \text{ W cm}^{-2}$), which is roughly the saturation intensity for ionization (see, for example, Fig. 2); the dashed curve is for $5 \times 10^{14} \text{ W cm}^{-2}$, which corresponds to a factor of 10 decrease in the ionization rate. For the 21st harmonic of argon [Fig. 1(b)] we also present two curves: the solid line is for the saturation intensity of $3 \times 10^{14} \text{ W cm}^{-2}$ and the dashed curve is for $2 \times 10^{14} \text{ W cm}^{-2}$, where the ionization rate is lower by a factor of 10 [8]. The agreement between the experiment and our simple theoretical estimate is very good. This suggests that the physical mechanism of the harmonic generation process is correctly described by the semiclassical picture drawn above.

Figure 1(c) presents our experimental data on the Ne^{2+} ion yield as a function of the ellipticity, measured with 625-nm light at peak intensity $I = 9 \times 10^{14} \text{ W cm}^{-2}$, where the “knee” in the Ne^{2+} yield is observed (Fig. 2). A striking feature of the dependence in Fig. 1(c) is that it approximately follows the ellipticity dependence of harmonic emission in Ne [Fig. 1(a)]. This experimental fact suggests that these two different physical phenomena indeed have a common underlying physical mechanism, as suggested in Ref. [3].

The quantum generalization [12] of the semiclassical model [3] discussed above only deals with harmonic generation. However, the experimental results on the ellipticity dependence of the Ne^{2+} ion yield can be quantitatively analyzed if we assume that the semiclassical model [3] correctly identifies correlated two-electron multiphoton ionization as an inelastic scattering even ($A^+ + e \rightarrow A^{2+} + 2e$).

Let us first estimate the *maximum* impact parameters contributing to this process. The energy transferred to the bound electron by the incident electron is estimated [13] as $\Delta \mathcal{E}_b = e^4 / (b^2 \mathcal{E}_i)$, where \mathcal{E}_i is the incident electron energy

and b is the impact parameter. Taking both $\Delta\mathcal{E}_b$ and \mathcal{E}_i as the binding energy of the second electron, $\Delta\mathcal{E}_b = \mathcal{E}_i = I_p^+$, we see that the maximum impact parameters which can contribute to the process are on the order of one Bohr radius. This value is much smaller than the size of the continuum wave packet $|\Psi_c(x,t)|^2$; its full width at half maximum is typically $L \sim 20 \text{ \AA}$ at the moment of return to the nucleus. We can therefore make an estimate for the relative strength of the e - $2e$ ionization signal as a function of ellipticity by measuring the relative number of electrons passing the origin within $b_0 \sim 1$ a.u. Since $L \gg b_0$, the result is independent of the exact choice of b_0 and is fully determined by the electron density in the continuum at the origin, $|\Psi_c(t, \mathbf{x}=\mathbf{0})|^2$.

We have calculated the ratio $R_i(t) = |\Psi_c(t, \mathbf{x}=\mathbf{0}, \varepsilon)|^2 / |\Psi_c(t, \mathbf{x}=\mathbf{0}, \varepsilon=0)|^2$, using the wave function $\Psi_c(t, \mathbf{x}, \varepsilon)$ found in Ref. [12]. This ratio is time dependent and, as discussed above for harmonics, each moment of time t^* is associated with an energy $\mathcal{E}(t^*)$, which an electron born at rest near the origin has if it comes back at the moment t^* . In Fig. 1(c) we plot $R_i(t)$ for two moments of time t^* , corresponding to the maximum possible energy of the returning electron $\mathcal{E}(t^*) = 3.17U_p$ (i.e., $t^* \approx 4.3/\omega$, dashed curve) and to the energy equal to the binding energy of a second electron (solid curve).

As seen in Fig. 1(c), our estimate turns out to be in very good agreement with experimental data. This fact, together with very similar dependence of high-harmonic yield and Ne^{2+} yield as a function of ellipticity supports our assumption that both processes have a common underlying physical mechanism.

The semiclassical model [3] has only one free parameter, the transverse spread of the electron wave function. The data presented in Fig. 1 remove this freedom and therefore we can

estimate the absolute yield of Ne^{2+} vs laser intensity. We have approximated the e - $2e$ cross section in a strong laser field by its field-free value $\sigma_0(\mathcal{E})$. Since, at the laser intensities we are dealing with, the electron collisionally excited (really or virtually) to any excited state will be immediately ionized, one should expect that $\sigma_0(\mathcal{E})$ underestimates the correct value of the cross section, as it neglects the possibility of real or virtual excitation. Using published cross-section data [14], ADK tunneling rates to calculate ionization probabilities and classical trajectory calculations to determine the velocity distribution of electrons passing the ion, we obtain the solid curves shown in Fig. 2. The deviation between experiment and theory most probably results from the assumption that $\sigma(\mathcal{E}) = \sigma_0(\mathcal{E})$.

In conclusion, we have used two different diagnostics of the strong-field light-matter interaction. We find that the results are quantitatively consistent with a quantum-mechanical model of strong-field light-atom interactions [12]. Both the model and experiment are consistent with the predictions of the semiclassical theory. Another explanation of high-field correlated-two-electron multiphoton ionization involving shake-off has been proposed [4], but to our knowledge there have been no predictions of ellipticity dependence from this model. Correlated two-electron multiphoton processes were originally found [5] in much lower power experiments where Keldysh-like models are inappropriate. We think that here careful studies of the ellipticity dependence would also help to elucidate the basic mechanism.

The authors would like to thank Dr. A. Bandrauk, Dr. M. Lewenstein, Dr. A. Stolow, Dr. D. Villeneuve, and Dr. A. Zavrinyev for many helpful discussions. The technical support of D. Joines and D. Roth was of great value.

-
- [1] J. J. Macklin, J. D. Kmetc, and C. L. Gordon III, *Phys. Rev. Lett.* **70**, 766 (1993), and references within.
- [2] A. L'Huillier *et al.*, in *Atoms in Intense Fields*, edited by M. Gavrila (Academic, New York, 1992), pp. 139–206.
- [3] P. B. Corkum, *Phys. Rev. Lett.* **71**, 1994 (1993).
- [4] D. N. Fittinghoff *et al.*, *Phys. Rev. Lett.* **69**, 2642 (1992).
- [5] A. L'Huillier *et al.*, *Phys. Rev. A* **27**, 2503 (1983).
- [6] P. B. Corkum, N. H. Burnett, and F. Brunel, *Phys. Rev. Lett.* **62**, 1259 (1989).
- [7] S. Augst *et al.*, *Phys. Rev. Lett.* **63**, 2212 (1989).
- [8] M. V. Ammosov, N. B. Delone, and V. P. Krainov, *Zh. Eksp. Teor. Fiz.* **91**, 2008 (1986) [*Sov. Phys. JETP* **64**, 1191 (1986)].
- [9] K. S. Budil *et al.*, *Phys. Rev. A* **48**, R3437 (1993).
- [10] C. Rolland and P. B. Corkum, *Opt. Commun.* **59**, 64 (1986).
- [11] K. C. Kulander, K. J. Schafer, and J. L. Krause, in *Super-Intense Laser-Atom Physics*, edited by B. Piraux, A. L'Huillier, and K. Rzazewski (Plenum, New York, 1994), p. 95.
- [12] M. Lewenstein *et al.*, *Phys. Rev. A* **49**, 2117 (1994); A. L'Huillier *et al.*, *ibid.* **48**, R3433 (1993).
- [13] J. Jackson, *Classical Electrodynamics* (Wiley, New York, 1962), p. 431.
- [14] H. Tawara and T. Kato, *At. Data Nucl. Data Tables* **36**, 167 (1987).